Characteristics of cooling water fouling in a heat exchange system

Sun-Kyung Sung[1,*], Sang-Ho Suh[2] and Dong-Woo Kim[3]

[1]*Dept. of Building Equipment System Engineering, Kyungwon University , Sungnam Kyonggi 461-702, Korea*
[2]*Dept. of Mechanical Engineering, Soongsil University, Seoul 156-743, Korea*
[3]*Dept. of Building Technology, Suwon Science College, Hwasung, Kyonggi 445-742, Korea*

Abstract

This study investigated the efficiency of the physical water treatment method in preventing and controlling fouling accumulation on heat transfer surfaces in a laboratory heat exchange system with tap and artificial water. To investigate the fouling characteristics, an experimental test facility with a plate type heat exchange system was newly built, where cooling and hot water moved in opposite directions forming a counter-flow heat exchanger. The obtained fouling resistances were used to analyze the effects of the physical water treatment on fouling mitigation. Furthermore, the surface tension and pH values of water were also measured. This study compared the fouling characteristics of cooling water in the heat exchange system with and without the mitigation methods for various inlet velocities. In the presence of the electrode devices with a velocity of 0.5m/s, the fouling resistance was reduced by 79% compared to that in the absence of electrode devices.

Keywords: Fouling; Fouling factor; Precipitation fouling; Physical water treatment; Heat exchange system; Anti-fouling technology

---

1. Introduction

In the areas of air-conditioning systems for buildings and refrigeration or heat pump systems for industries, it is necessary to use the coolant for removing the heat generated from the condensing process. In general, tap water is used as the coolant for buildings, underground water is used for industries, and river water is used for district heating companies. However, for the cases of using the tap water and underground water, the coolant is usually sent to a cooling tower and is re-circulated after cooling down the heat by evaporating the water at the tower. In a re-circulating cooling system, concentration of mineral ions in water continuously increases due to water evaporation. When the concentrated water is heated inside heat transfer equipment, the calcium and bicarbonate ions precipitate due to the changes in solubility, forming

hard scale on the heat-transfer surfaces, and clogging pipes and manifolds.

Fouling is defined as scale deposit layer such as the formation of calcium carbonate on heat transfer surfaces and occurs more rapidly when the concentrated water is circulated in the cooling towers and heat exchangers. The economic loss due to the fouling is one of the biggest problems in all industries dealing with heat-transfer equipment. It is very important to secure anti-fouling technology on the surfaces of heat exchange systems in order to reduce carbon dioxide products and utilize energy efficiently. Besides, as the fouling deposited on the heat transfer surfaces reduces the cross sectional areas of the flow passages, the flow rate of the coolant decreases and the pressure loss of the system increases [1].

Even though there are several researches reported in the worldwide open literature regarding improving the heat transfer rates of the heat exchange system against fouling, a complete solution is yet to come [2-4].

---
[*]Corresponding author. Tel.: +82 31 750 5883, Fax.: +82 31 750 5314
E-mail address: sksung@kyungwon.ac.kr

Domestically, researches related to the heat exchange system are focused only on structures of the heat exchanging system to improve the heat transfer efficiency. In the late 1990's, the need for research on fouling were proposed but the number of publications was limited [5].

The objectives of this study were to investigate the characteristics of cooling water fouling in the heat exchange system depending on the two kinds of water as a coolant and to compare the fouling accumulation on heat transfer surfaces in the presence and the absence of the mitigation devices for various inlet velocities.

2. Fouling

2.1 Fouling

When any undesirable material is deposited on a heat exchanger surface, it is traditionally called fouling [6], and it is further classified into precipitation fouling, particulate fouling, chemical reaction fouling, corrosion fouling, biological fouling, and freezing fouling. In general, the fouling that occurs in industrial heat exchange systems is due to precipitation fouling.

Fig. 1 shows the heating process of salt solution solubility. Since the inlet temperature of the coolant flowing through the heat exchange system is varying, its solubility is also changed. As the temperature of the salt solution (T_1) increases along the saturation curve, precipitation fouling occurs when the solubility exceeds the saturation temperature (T_s) [7].

Water qualities of cooling water causing fouling are $CaCO_3$, $BaSO_4$, $CaSO_4$, Silica, and Fe. Since domestic city water contains calcium ions, the major precipitation fouling part is $CaCO_3$ when tap water is
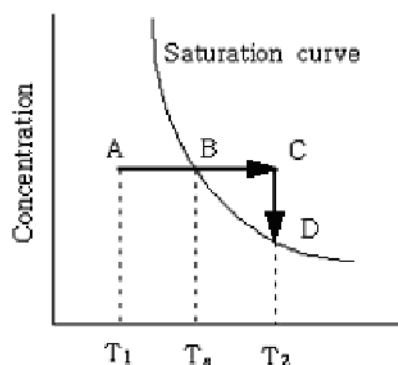

Fig. 1. A heating process of salt solution solubility.

used as a coolant in a heat exchanger [8].

2.2 Fouling resistance

The fouling resistance, R_f, can be expressed as follows:

$$R_f = \frac{1}{U_f} - \frac{1}{U_c} \qquad (1)$$

Where U_f is the heat transfer coefficient in the presence of the fouling, and U_c is the heat transfer coefficient in the absence of the fouling. These heat transfer coefficients are calculated as follows:

$$U = \frac{\dot{Q}}{A\Delta T_{LMTD}} \qquad (2)$$

Where A is the cross sectional area of the flow and ΔT_{LMTD} is the logarithmic mean temperature difference defined as below.

$$\Delta T_{LMTD} = \frac{\left(T_{h,i} - T_{c,o}\right) - \left(T_{h,o} - T_{c,i}\right)}{\ln\left[\dfrac{T_{h,i} - T_{c,o}}{T_{h,o} - T_{c,i}}\right]} \qquad (3)$$

The amount of the heat transfer rate, $\dot{Q}$, can be calculated as follows.

$$\dot{Q} = \left[\dot{m} C_p \left(T_i - T_o\right)\right]_h = \left[\dot{m} C_p \left(T_o - T_i\right)\right]_c \qquad (4)$$

In Eqs. (3) and (4), ΔT_{LMTD} and $\dot{Q}$ are calculated from the measured temperatures of the heat exchanger's inlet and outlet and the measured volumetric flow rates. Those of the heat exchanger's temperatures are measured by thermocouples and then converted into different voltage values by using an A/D board. With the use of Visual Basic and Excel, ΔT_{LMTD} and $\dot{Q}$ are calculated from the converted voltage values. Finally, the fouling resistance, R_f, in Eq. (1) is evaluated from the relationship of Eq. (2).

3. Experimental setup

3.1 Experimental water

Because the quality of water affects fouling differently, the selection of the water for the experiment is very important. In this study, tap water and artificial water were chosen. Compared with the waters in Europe and America, the domestic water has less hardness [9]. Since the low hardness of water results in slow fouling, this study used hard water with high

concentration to reduce the required experimental time.

This study focused on the water circulating through the cooling tower. The tap water completed the concentration process by circulating through the cooling tower until 2,000 µS/cm of the electrical conductivity achieved was used. However, due to the longer experimental time, artificial water added with chemicals was also used instead of the direct use of the tap water [10]. $CaCl_2$ of 0.669 g and $NaCO_2$ of 0.784 g were artificially added into 1 liter of the tap water. The waters used were carefully analyzed before and after the experiments. With the use of EDTA (Ethylene Diamine Tetraacetic Acid), total hardness, calcium hardness, alkalinity, and chloride of the water were analyzed. Also, the electrical conductivity and the pH value of water were measured.

3.2 Experimental apparatus

To investigate the fouling characteristics in a heat exchange system, an experimental test apparatus with a plate type heat exchanger was newly built. A schematic diagram of the fouling test apparatus is shown in Fig. 2. This experimental setup consists of the water concentration adjustment part and the fouling forming part.

The water concentration adjustment part included a cooling tower, an electrical heater, a hot-water supplying pump, a cold-water supplying pump, an electrical conductivity meter, a heat exchanger, a large water reservoir, flow meters, and several valves. To increase the water concentration, the water flowing through the electrical heater was evaporated at the cooling tower and then new water was added.

The fouling forming part consisted of a copper plate as a heat-transfer surface, an observation window, a cooling-water channel, and a hot-water channel. The effective roughness of the copper plate used was 1.5 µm. The cooling water and hot water flowed in opposite directions, thus forming a counter-flow heat exchanger. In order to accelerate the fouling process, a high heat flux was used and the water concentration was increased to 2,000 µmhos/cm.

To visualize the formation of fouling on the heat transfer surface, real time images were obtained by using a CCD camera with microscopy (×40). X-ray diffraction method was also used to characterize fouling structures. Fouling resistances and overall heat transfer coefficients were experimentally measured to examine fouling characteristics.
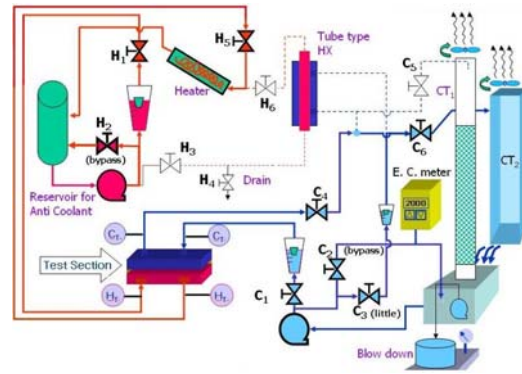

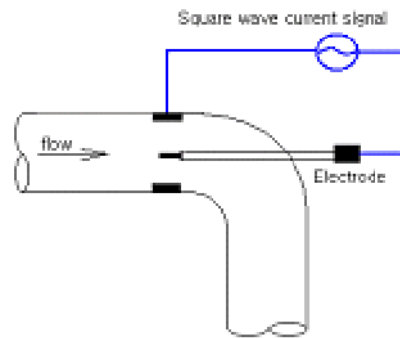Fig. 2. Schematic diagram of the experimental apparatus.

Fig. 3. Schematic diagram of the metal electrode device.

Temperatures at the inlet and outlet of the test section were measured by four thermocouples and recorded by an A/D board in real-time. The inlet temperature of the cold water was maintained at 30±0.5 °C by a cooling fan at the cooling tower. However, the inlet temperature of the hot water was regulated at 95±0.5 °C by an electrical heater. The flow velocity of cooling water in the test section was changed in a range of 0.5-1.5 m/s, while the velocity of hot water was fixed at 3 m/s.

In this study, the low voltage method was adopted to investigate the effects of fouling mitigation devices with metal and carbon electrode devices on the prevention of fouling. Fig. 3 shows a schematic diagram of the metal electrode device and Fig. 4 shows the ring-type graphite electrode device. The graphite electrode device has two rings. Inner and outer diameters of the rings are 9.5 mm and 18mm. The distance between two rings is 12 mm. These electrode devices were installed at the inlet of the heat exchange system. Fig. 5 shows 12 volts of the square wave signal supplied into the electrode devices. The current supplied into the electrodes was maintained at 2.5 mA by a
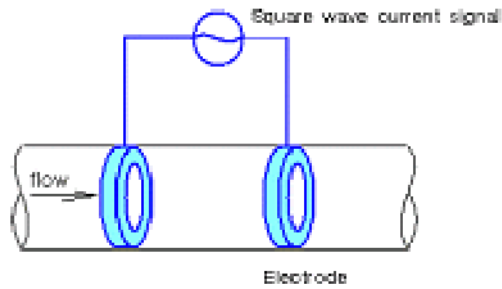
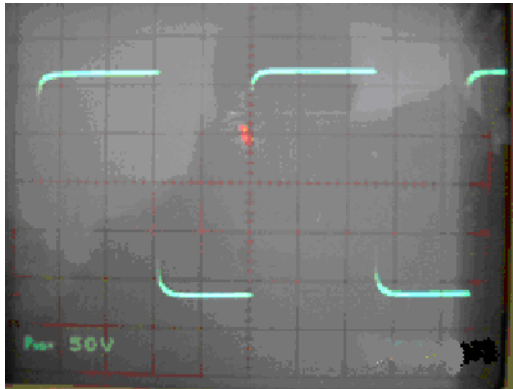Fig. 4. Schematic diagram of the graphite electrode device.

Fig. 5. 12 volts of square wave signal captured by an oscilloscope for electrode devices.

Table 1. Properties of the water samples.

	Tap water	Tap water (hard water)	artificial water
Conductivity (μ S/cm)	158	2000	1400
pH	7.4	8.3	7.7
Ca Hardness (mg/ℓ)	50	640	220
Mg Hardness (mg/ℓ)	12	130	10
Total Hardness (mg/ℓ)	62	770	230
Alkalinity (mg/ℓ)	40	185	250
Chloride (mg/ℓ)	26	340	380

4.2 Fouling formation with and without the anti-fouling devices

Using the experimental setup specified in Fig. 2, fouling was formed according to the tap and artificial waters. About 300 hours of the experimental time was required for the tap water and 100 hours was required for the artificial water. As can be seen from Fig. 6, the fouling coefficients were about 1.23×10^{-4} m^{2}K/W for 0.5 m/s, 3.53×10^{-5} m^{2}K/W for 1.0 m/s, and 1.53×10^{-5} m^{2}K/W for 1.5 m/s. As the flow velocity increased, the fouling coefficient sharply decreased. Fig. 7 shows the variations of the fouling coefficient according to the different flow velocities for the artificial water. The fouling coefficients after 25 hours were about 9.83×10^{-5} m^{2}K/W for 0.5 m/s, 1.83×10^{-5} m^{2}K/W for 1.0 m/s, and 0.33×10^{-5} m^{2}K/W for 1.5 m/s. Similarly, as can be seen from the results obtained by the tap water, the fouling coefficient decreased as the flow velocity increased. When the flow velocity is high, some of the particles that arrive at a surface fail to stick and return to the bulk flow. Whereas, some particles hit the surface and rebound into the flow by a removal mechanism. Therefore, the fouling coefficient decreases as the flow velocity increases. The above fouling coefficients were mean overall averaged values since the fouling on the surface might not be formed uniformly.

Figs. 8 to 11 show the effects of fouling mitigation for tap and artificial waters depending on the different flow velocities. For a flow velocity of 0.5 m/s, the fouling resistance of tap water was 1.223×10^{-4} m^{2}K/W in the absence of the anti-fouling device and 2.573×10^{-5} m^{2}K/W with the metal electrode device after 250 hours. The fouling coefficient was decreased by approximately 79% with the use of electrode device in Fig. 8. However, for a flow velocity of

variable resistance and the input frequency was 1,100 Hz.

4. Experimental results and discussion

4.1 Water analyses

Depending on the water used, Table 1 shows the results of the water analyses. Tap water was taken at the experimental laboratory and hard water was concentrated in a cooling tower. As can be seen from Table 1, the electrical conductivity and the total hardness of the tap water were 158 μS/cm and 62 mg/*l*, and those values of the hard water were 2,000 μS/cm and 770 mg/*l*. The electrical conductivity and the total hardness of the hard water were increased about 12 times than those of the tap water by the concentration process. For the artificial water, the electrical conductivity and the total hardness were about 1,400 μS/cm and 230 mg/*l*.
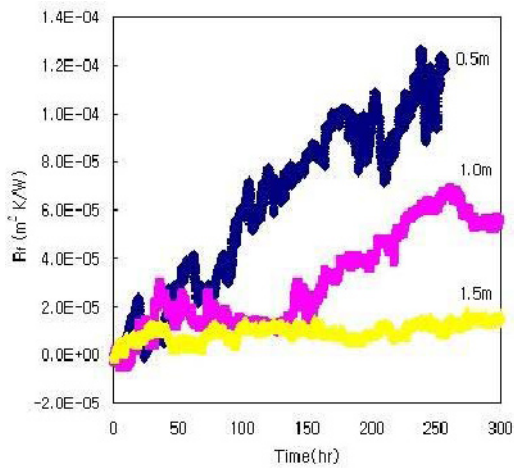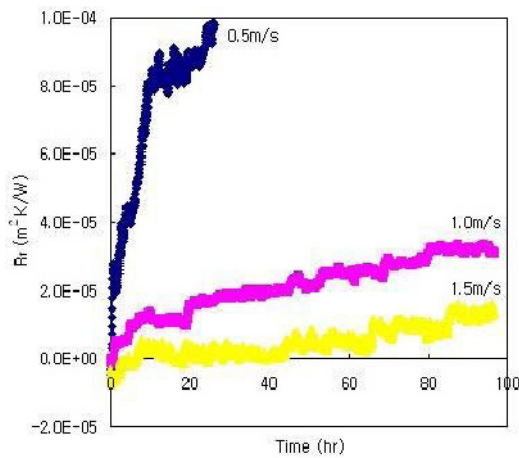
Fig. 6. Variations of the fouling coefficient for tap water.

Fig. 7. Variations of the fouling coefficient for artificial water.

1.0 m/s, the fouling resistance was 6.643×10^{-5} m^{2}K/W without the anti-fouling device and 2.433×10^{-5} m^{2}K/W with the metal electrode device in Fig. 9. As the flow velocity increased, the effect of fouling mitigation slightly reduced. With the use of the artificial water, the fouling resistances were 9.83×10^{-5} m^{2}K/W in the absence of the anti-fouling device, 3.83×10^{-5} m^{2}K/W with the metal electrode device, and 6.33×10^{-5} m^{2}K/W with the graphite electrode device for the flow velocity of 0.5 m/s after 26 hours in Fig. 10. For a flow velocity of 1.0 m/s, the fouling resistances were 3.33×10^{-5} m^{2}K/W in the absence of the anti-fouling device, 2.143×10^{-5} m^{2}K/W with the metal electrode device, and 2.623×10^{-5} m^{2}K/W
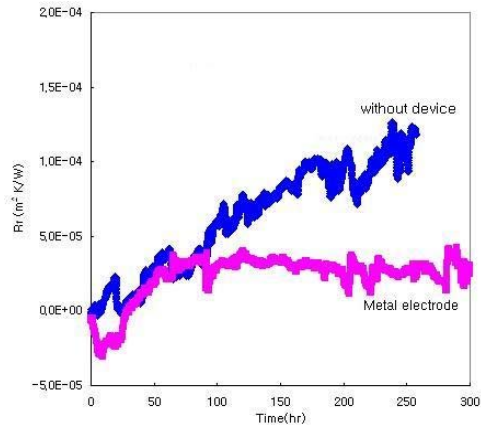

Fig. 8. Variations of the fouling coefficient for tap water with the electrode mitigation device (average velocity, 0.5 m/s).
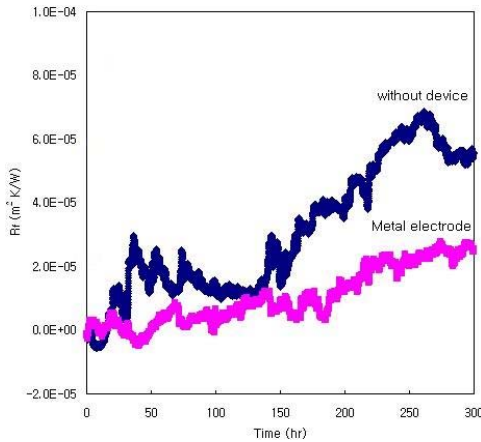

Fig. 9. Variations of the fouling coefficient for tap water with the electrode mitigation device (average velocity, 1.0 m/s).
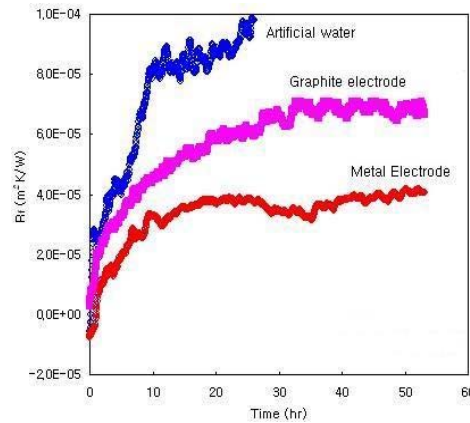

Fig. 10. Variations of the fouling coefficient for artificial water with/without the electrode mitigation devices (average velocity, 0.5 m/s).
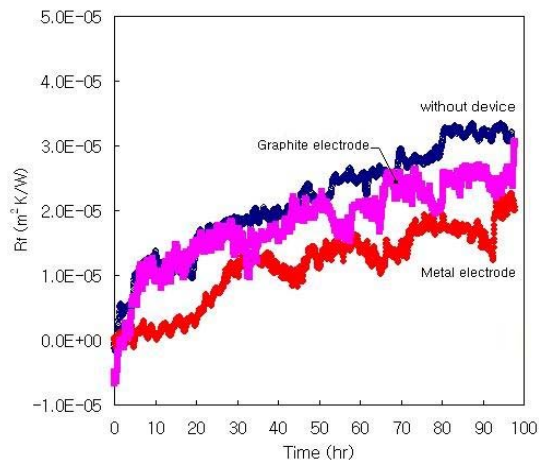
Fig. 11. Variations of the fouling coefficient for artificial water with/without the electrode mitigation devices (average velocity, 1.0 m/s).

with the graphite electrode device in Fig. 11. The fouling resistances for the metal and graphite electrode devices were decreased by about 35% and 21%, respectively. It was found that the electrode fouling prevention devices reduced the formation of aragonite calcium carbonate compared to the case of the absence of mitigation devices.

4.3 pH variations

Several researchers found that the value of pH affected the results of the fouling. As the value of pH increased, the amount of the precipitation fouling decreased. While the value of pH decreased, the amount of the precipitation fouling increased [11]. Since a decrease in pH value increases the solubility of $CaCO_3$, the tendency of $CaCO_3$ precipitation can be indirectly estimated by monitoring pH changes in water. Thus, the effects of fouling mitigation devices could be evaluated by measuring the variations of the pH values.

To investigate the effects of pH on the fouling, the pH values were measured according to the numbers of cooling water circulations through the fouling mitigation device as was shown in Fig. 12. The number of circulations was calculated by dividing the total amount of the cooling water flowing through the fouling mitigation device into the amount of water at the large water reservoir. During these measurements, the velocity at the fouling mitigation devices was controlled at 1 m/s. The pH values were measured at two

Table 2. Variations of pH according to the number of the cooling water circulation.

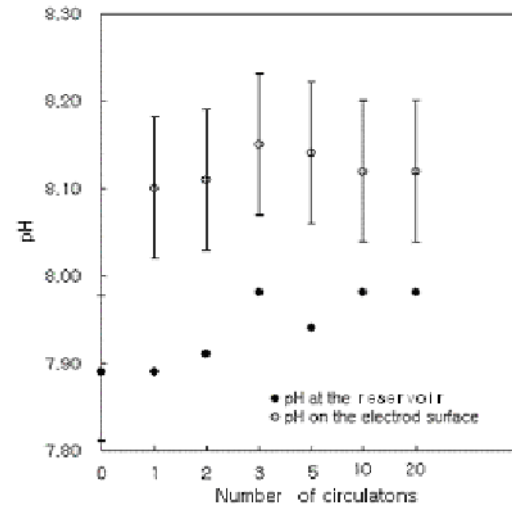| Number of circulation	pH at the reservoir	pH at the electrode surface
0	7.89	7.89
1	7.89	8.10
2	7.91	8.11
3	7.98	8.15
5	7.94	8.14
10	7.98	8.12
20	7.98	8.13

Fig. 12. Variations of pH according to the number of cooling water circulations.

different locations. One was at the cooling water reservoir and the other was at the electrode surface of the fouling mitigation device. To measure the pH at the electrode surface, a needle having a diameter of 0.7 mm was installed at 0.5 mm above the electrode surface. Then the surface water was taken from the needle that was parallel to the flow direction.

Table 2 and Fig. 12 show the variations of the pH at the two locations. The values of pH at the water reservoir gradually increased after the first circulation and then maintained the same values after three times of the cooling water circulations. The values of pH at the electrode surface largely increased as soon as the cooling water circulated through the fouling mitigation devices, and then maintained the same values after three circulations of the cooling water. It could be concluded that the precipitation fouling decreased with the fouling mitigation devices since the pH val-

ues largely increased as soon as the cooling water circulated.

4.4 Surface tension variations

Surface tension is a property of the liquid and depends on the other fluid in contact with it at the interface. The surface energy of a liquid-liquid state is less than that of a solid-liquid state in water [12]. Hence, the surface energy at the interface of water molecules and the glass tube is much bigger than that of between two water molecules. However, as the number of the colloidal particles increases in the water, the surface energy at the interface of water molecule and colloidal particles increases. In other words, the surface energy at the interface between water molecule and glass tube decreases relatively. Therefore, the surface tension of the water decreases as the number of colloidal particles increases in the water. The colloidal particles that led to bulk precipitation might have reduced the fouling on the surface. Thus, it is possible to predict the fouling mitigation effects by measuring the surface tension.

Fig. 13 depicts a schematic diagram of a capillary tube system to measure the surface tension of water, and Table 3 shows the results of the water surface tensions measured after passing through the graphite electrodes. In Table 3, ρ is the density of water, h and R denote the height of the water column and the radius of the capillary tube and σ is the surface tension, defined by Equation (5):

$$\sigma = \rho g h R / 2 \qquad (5)$$

To measure the surface tension of water accurately, the height of water in the Pyrex glass capillary tube inserted into sample was recorded. The diameter of the capillary tube was 1.15 mm and the length was 100 mm. The end of the capillary tube has sharp edges to reduce the interfacial force and it was inserted about 5 mm beneath the water surface by a height control screw to measure the liquid level. Since the surface tension depended on the temperature, the temperature of the tested water was maintained at 25 °C.

The uncertainty analysis for the height of the water column measurements in Table 3 showed about ±1% error. As can be seen from the table, the surface tension of the artificial water decreased with the increase of the circulation. Thus, the fouling mitigation device

Table 3. Results of the surface tension measurements for artificial water with the numbers of the circulation (graphite electrode).

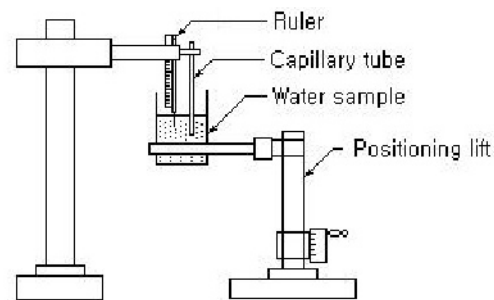| Numbers of circulation (0.5 m/s)	h (mm)	ρ (kg/m³)	R (m)	σ (N/m)	Reduction rate (%)
0	25.6	997.1	0.00057	0.07133	0.0
1	25.4	997.1	0.00057	0.07077	0.78
2	25.0	997.1	0.00057	0.06966	2.3
3	25.0	997.1	0.00057	0.06966	2.3
5	24.3	997.1	0.00057	0.06771	2.1
10	23.2	997.1	0.00057	0.06465	9.4
20	23.0	997.1	0.00057	0.06401	10.2

Fig. 13. Schematic diagram of the surface tension measurements.

might have reduced the fouling resistance through bulk precipitation.

5. Conclusions

This study suggested fouling mitigation methods by using electrode devices. This study investigated the efficiency of the fouling mitigation devices in preventing and controlling fouling accumulation on heat transfer surfaces in the laboratory heat exchange system with tap and artificial water. Fouling coefficients, pH values, and surface tensions of the cooling water were experimentally measured with and without the mitigation devices for various inlet velocities. Based on these experimental results, this study suggests the following.

(1) With the use of the tap and artificial waters, the fouling coefficients were strongly dependent on the velocity of the flow since the fouling resistances were sharply increased as the flow velocity changed from 1.0 m/s to 0.5 m/s.

(2) For a flow velocity of 0.5 m/s, the fouling coefficients of the tap water were decreased by about 79%

after 250 hours with the use of the electrode device. However, for a flow velocity of 1.0 m/s, the fouling coefficients were decreased by about 63%.

(3) For a flow velocity of 0.5 m/s, the fouling coefficients were decreased by about 61% in the metal electrode device, and 36% in the graphite electrode device with the use of artificial water. For a flow velocity of 1.0 m/s, the fouling coefficients in the metal and graphite electrode devices were decreased by about 35% and 21%, respectively.

(4) The precipitation fouling decreased with the fouling mitigation devices since the pH values largely increased as soon as the cooling water circulated through the mitigation device.

(5) The surface tension of the artificial water decreased due to the increase of the flow circulation. Thus, the fouling mitigation device reduced the fouling resistance through the bulk precipitation.

References

[1] T. R. Bott, The Fouling of Heat Exchangers, Elsevier Science, New York, (1995)

[2] Y. I. Cho and B. G. Choi, Validation of an electronic anti-fouling technology in a single-tube heat exchanger, *International Journal of Heat and Mass Transfer*, 42, (1999) 1491-1499.

[3] M. Forster, W. Augustin and M. Bohnet, Influence of the adhesion force crystal/heat exchanger surface on fouling mitigation, *Chemical Engineering and Processing,* 38 (1999) 449-461.

[4] K. J. Kronenberg, Experimental evidence for effects of magnetic fields on moving water, *IEEE Transactions on Magnetics, MAG-21* (1985) 2059-2061.

[5] Y. P. Lee, S. Y. Yoon, J. S. Jung and N. H. Kim, Mechanism of fouling reduction and heat transfer enhancement in a circulating fluidized bed heat exchanger, *Trans. of SAREK*, 7 (3) (1995) 450-460.

[6] D. Hasson, M. Avriel, W. Resnick, T. Rozenman and S. Windreich, Mechanism of calcium carbonate scale deposition on heat-transfer surface, *Ind. Eng. Chem. Fund*., 7 (1968) 58-63.

[7] W. T. Kim and Y. I. Cho, Experimental study of the crystal growth behavior of $CaCO_3$ fouling using a microscope, *Experimental Heat Transfer*, 13 (2000) 153-161.

[8] S. K. Sung, S. H. Suh and H. W. Roh, "Analyses of fouling mechanism using visualization techniques in a Lab-scale plate-type heat exchanging system, *Trans. of SAREK*, 16 (4) (2004) 349-354.

[9] S. K. Sung, S. H. Suh and H. W. Roh, A study on the formation of fouling in a heat exchanging system for river water, *Trans. of KSME*, 28 (6) (2004) 646-651.

[10] Qingfeng Yang, Yangqiao Liu, Anzhong Gu, Jie Ding and Ziqiu Shen, Investigation of induction period and morphology of $CaCo_3$ fouling on heated surface, *Chemical Engineering Science 57*, (2002) 921-931.

[11] I. H. Newson, G. A. Miller, J. W. Haynes, T. R. Bott and R. D. Williamson, Particulate fouling: studies of deposition, removal and sticking mechanism in a haematite/water system, *2nd Nat. Heat Trans. Conf*. Glasgow, I . Mech. E. (1988) 137-160.

[12] K. J. Mysels, Introduction to Colloid Chemistry, Interscience Publishers, Inc., New York, (1976) 184-187.